

AD-A058 983

AIR FORCE GEOPHYSICS LAB HANSCOM AFB MASS
SPACECRAFT CHARGING AT GEOSYNCHRONOUS ORBIT - SOLUTION FOR ECLI--ETC(U)

UNCLASSIFIED

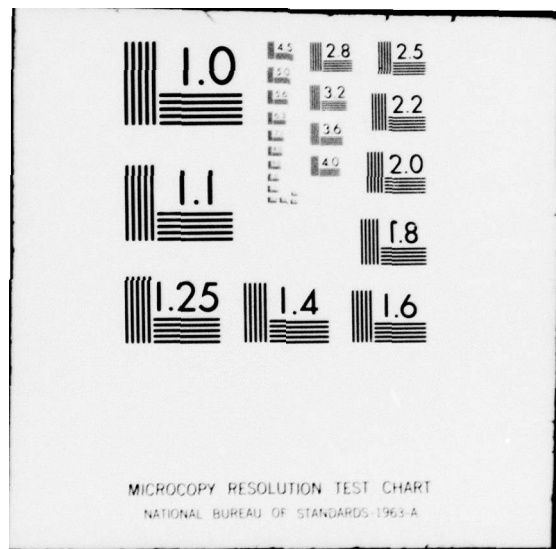
AFGL-TR-78-0122

F/6 20/3

NL

| OF |
AD
A058983

END
DATE
FILMED
11-78
DDC



AD A058983

DDC FILE COPY

14 AFGL-TR-78-0122 AFGL-AFSC-389

AIR FORCE SURVEYS IN GEOPHYSICS, NO. 389

9

12



LEVEL II

6 Spacecraft Charging at Geosynchronous Orbit – Solution for Eclipse Passage.

10

HENRY BERRY GARRETT CAPT, USAF

ALLEN G. RUBIN

9 Determined, 1/1

11

15 May 78

12

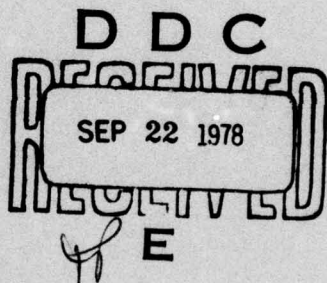
17 P.

16

7661

17

48



Approved for public release; distribution unlimited.

SPACE PHYSICS DIVISION PROJECT 7661
AIR FORCE GEOPHYSICS LABORATORY
HANSCOM AFB, MASSACHUSETTS 01731

AIR FORCE SYSTEMS COMMAND, USAF



78 09 21 002

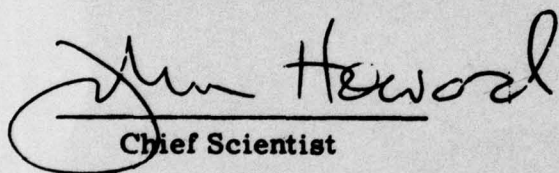
409578

mt

This report has been reviewed by the ESD Information Office (OI) and is releasable to the National Technical Information Service (NTIS).

This technical report has been reviewed and is approved for publication.

FOR THE COMMANDER



John Howard
Chief Scientist

Qualified requestors may obtain additional copies from the Defense Documentation Center. All others should apply to the National Technical Information Service.

Unclassified

SECURITY CLASSIFICATION OF THIS PAGE (When Data Entered)

REPORT DOCUMENTATION PAGE			READ INSTRUCTIONS BEFORE COMPLETING FORM
1. REPORT NUMBER AFGL-TR-78-0122	2. GOVT ACCESSION NO.	3. RECEIPT'S CATALOG NUMBER	
4. TITLE (and Subtitle) SPACECRAFT CHARGING AT GEOSYNCHRONOUS ORBIT - SOLUTION FOR ECLIPSE PASSAGE		5. TYPE OF REPORT & PERIOD COVERED Scientific. Interim.	
7. AUTHOR(s) Henry Berry Garrett, Capt, USAF Allen G. Rubin		8. CONTRACT OR GRANT NUMBER(s)	
9. PERFORMING ORGANIZATION NAME AND ADDRESS Air Force Geophysics Laboratory (PHG) Hanscom AFB Massachusetts 01731		10. PROGRAM ELEMENT, PROJECT, TASK AREA & WORK UNIT NUMBERS 62101F 76610801	
11. CONTROLLING OFFICE NAME AND ADDRESS Air Force Geophysics Laboratory(PHG) Hanscom AFB Massachusetts 01731		12. REPORT DATE 15 May 1978	
14. MONITORING AGENCY NAME & ADDRESS(if different from Controlling Office)		13. NUMBER OF PAGES 17	
		15. SECURITY CLASS. (of this report) Unclassified	
		15a. DECLASSIFICATION/DOWNGRADING SCHEDULE	
16. DISTRIBUTION STATEMENT (of this Report) Approved for public release; distribution unlimited.			
17. DISTRIBUTION STATEMENT (of the abstract entered in Block 20, if different from Report)			
18. SUPPLEMENTARY NOTES			
19. KEY WORDS (Continue on reverse side if necessary and identify by block number) Plasma interactions Spacecraft charging Satellite anomalies			
20. ABSTRACT (Continue on reverse side if necessary and identify by block number) Rapid variations in spacecraft potential are observed on entry and exit from the earth's shadow. Generalized equations, based on elementary plasma probe theory, are developed which make quantitative estimates of these potentials as a function of satellite position in the earth's penumbra, and are compared with data from the ATS-5 and ATS-6 geosynchronous satellites. The agreement between the observations and the predictions results from the approximate constancy of the ratio of the ambient ion to electron current			

DD FORM 1473 EDITION OF 1 NOV 65 IS OBSOLETE

Unclassified

SECURITY CLASSIFICATION OF THIS PAGE (When Data Entered)

78 09 21 002

Unclassified

SECURITY CLASSIFICATION OF THIS PAGE(When Data Entered)

20. Abstract (Continued)

during injection events. Due to the significant size and shape differences of the ATS-5 and ATS-6 satellites, the results are applicable in many space physics situations such as estimating the effects of electron beams on satellite potential and of spacecraft charging on very large space structures.

Unclassified

SECURITY CLASSIFICATION OF THIS PAGE(When Data Entered)

Preface

The authors would like to thank Drs. W. Burke, E.C. Whipple, A.J. Dessler, W. Olson, and D. Hardy for their comments. C. Pike provided the impetus and encouragement for the study. Ms. J. Fink prepared the data for analysis. Dr. S.E. DeForest provided the ATS-5 and ATS-6 data and spent many invaluable hours explaining its use and interpretation.

ACQUISITION FOR		
WWD	White Section <input checked="" type="checkbox"/>	
DOC	Buff Section <input type="checkbox"/>	
UNANNOUNCED <input type="checkbox"/>		
JUSTIFICATION.....		
.....		
BY.....		
DISTRIBUTION/AVAILABILITY CODES		
DIST.	AVAIL. and/or SPECIAL	
A		

Contents

1. INTRODUCTION	7
2. BASIC EQUATIONS	7
3. POTENTIAL IN ECLIPSE	10
4. POTENTIAL DURING ECLIPSE PASSAGE	13
5. DISCUSSION	14
REFERENCES	17

Illustrations

1. The Altitude X_m Above the Earth of the Minimum Ray Path Between the Satellite and the Center of the Sun	10
2. The Observed Temperature of the Ambient Electrons vs the Satellite Potential in Eclipse	12
3. The Ratio of the Varying Potential to the Maximum Potential When the Spacecraft Were in Eclipse	14
4. The Occurrence Frequency of Eclipse Potentials for ATS-5 and ATS-6	16

Spacecraft Charging at Geosynchronous Orbit— Solution for Eclipse Passage

1. INTRODUCTION

The interactions between spacecraft and the ambient space environment have become an increasing problem to the space physics community. The best known of these environmental interactions is that resulting from spacecraft charge buildup (DeForest¹). In this report, simple plasma probe theory will be used to develop equations which allow estimations of the potential that exists between a spacecraft and the ambient medium in the presence of a varying photoelectron flux. The variations are compared with observations from the geosynchronous satellites ATS-5 and ATS-6.

2. BASIC EQUATIONS

The basic equation describing the spacecraft charging phenomenon is (Whipple,² and DeForest¹):

(Received for publication 11 May 1978)

1. DeForest, S. E. (1972) Spacecraft charging at synchronous orbit, J. Geophys. Res. 77:651-659.
2. Whipple, E. C. (1965) The Equilibrium Electric Potential of a Body in the Upper Atmosphere, NASA X-615-65-296.

$$J_E - (J_I + J_{SE} + J_{SI} + J_{BSE} + J_{PH}) = 0 \quad (1)$$

where

J_E = Incident electron current
 J_I = Incident ion current
 J_{SI} = Secondary electron current due to ions
 J_{SE} = Secondary electron current due to electrons
 J_{BSE} = Back-scattered electron current
 J_{PH} = Photoelectron current.

To first order, for the range of currents and potentials observed at geosynchronous orbit, the secondary and backscattered currents are approximated by linear relations:

$$J_{SE} \approx a J_E \quad (2)$$

$$J_{BSE} \approx b J_E$$

$$J_{SI} \approx c J_I$$

such that:

$$x J_E - y J_I - J_{PH} = 0 \quad (3)$$

for:

$$x = 1 - a - b$$

$$y = 1 + c .$$

From probe theory (Chen³) for a thick sheath around a spherical probe or in the absence of a sheath (DeForest¹), the current to a probe as a function of the ambient current and spacecraft potential for a negatively charged spacecraft is:

3. Chen, F. F. (1965) Electric Probes, Plasma Diagnostic Techniques, R. H. Huddlestome and S. L. Leonard (Ed.), Academic Press, Inc., New York, pp 113-200.

$$J_E(V) = J_{EO} e^{-|qV|/T_E} \quad (4)$$

$$J_I(V) = J_{IO} \left(1 + \frac{|qV|}{T_I} \right) \quad (5)$$

where

- V = Spacecraft potential in volts
- T_E = Maxwellian temperature of electrons in electron volts
- T_I = Maxwellian temperature of ions in electron volts
- q = Unit charge such that qV is in electron volts
- J_{EO} = Ambient electron current
- J_{IO} = Ambient ion current.

Eq. (3) becomes:

$$x J_{EO} e^{-|qV|/T_E} - y J_{IO} \left(1 + \frac{|qV|}{T_I} \right) - J_{PH} = 0 \quad (6)$$

J_{PH} , the photoelectron current, can be expressed as a function of the pre-eclipse photoelectron current, J_{PO} , and an attenuation function f representing the fraction of sunlight falling on the spacecraft. It is convenient to express this fraction in terms of the minimum altitude, X_m , for the ray between the satellite and the center of the sun (Figure 1). Thus Eq. (6) becomes:

$$\frac{|qV|}{T_I} = - \ln [(y/x)(J_{IO}/J_{EO})(1 + |qV|/T_I) + (1/x)(J_{PO}/J_{EO}) f(X_m)] \quad . \quad (7)$$

Equation (7) is the basic spacecraft charging equation in the presence of photoelectron emission. Assumptions will be made that reduce Eq. (7) to an analytic expression giving the spacecraft potential as a function of the electron temperature.

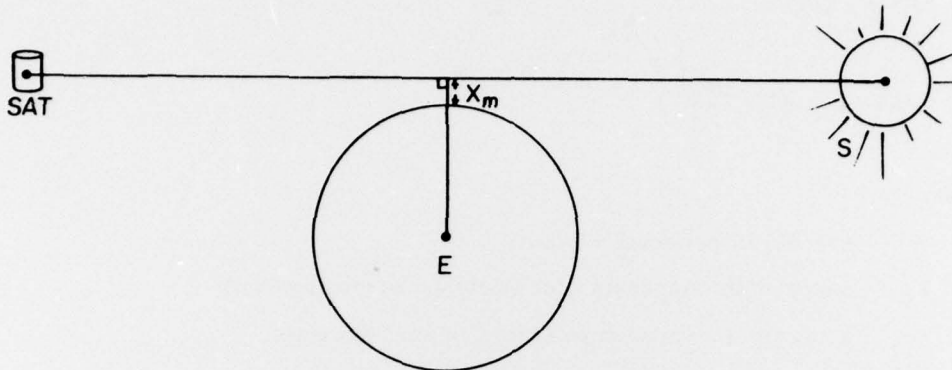


Figure 1. The Altitude X_m Above the Earth of the Minimum Ray Path Between the Satellite and the Center of the Sun

3. POTENTIAL IN ECLIPSE

When a spacecraft is in the earth's shadow, the photoelectron flux approaches zero (scattered light, moonlight, etc., may still be present) so that Eq. (7) becomes:

$$\frac{|qV_o|}{T_E} = - \ln \left[\left(\frac{y}{x} \right) \left(\frac{J_{IO}}{J_{EO}} \right) \left(1 + \frac{|qV_o|}{T_I} \right) \right] . \quad (8)$$

T_E , T_I , J_{IO} , and J_{EO} were calculated for 21 electron and ion spectra from ATS-5 and for four spectra from ATS-6 for intervals immediately preceding eclipse entry and immediately following exit from eclipse. These spectra cover the energy ranges 50 eV to 50 keV and 1 eV to 80 keV respectively (see DeForest and McIlwain,⁴ and Mauk and McIlwain⁵ for details).

Parameters x and y for the range of observed parameters are estimated from formulas given in Whipple² and Garrett⁶ to be:

4. DeForest, S. E., and McIlwain, C. E. (1971) Plasma clouds in the magnetosphere, *J. Geophys. Res.* 76:3587-3611.
5. Mauk, B. H., and McIlwain, C. E. (1975) ATS-6 UCSD auroral particles experiment, *IEEE Trans. Aerospace and Electronic Systems*, *AES-11*(No. 6): 1125-1130.
6. Garrett, H. B. (1978) Spacecraft Potential Calculations - A Model, AFGL-TR-78-0116.

$$a \approx 0.4 \quad (9)$$

$$b \approx 0.2$$

$$c \approx 3$$

Therefore:

$$x \approx 0.4 \quad (10)$$

$$y \approx 4$$

For the eclipse potentials corresponding to the 25 intervals, the ratio $|qV_o|/T_I$ is in general less than 1. Therefore, $\ln(1 + |qV_o|/T_I)$ is approximately 0. Equation 8 reduces to:

$$\frac{|qV_o|}{T_E} = \ln \left[\frac{1}{10} \left(\frac{J_{EO}}{J_{IO}} \right) \right] = \ln \left[\frac{1}{10} \left(\frac{n_E}{n_I} \right) \left(\frac{T_E}{T_I} \right)^{1/2} \left(\frac{m_I}{m_E} \right)^{1/2} \right] \quad (11)$$

where

n_E = Ambient electron density

n_I = Ambient ion density

m_E = Mass of electron

m_I = Mass of ion .

For the data studied, $T_I \approx 2.5 T_E$ and $n_E \approx n_I$ so that:

$$\frac{J_{EO}}{J_{IO}} = \left(\frac{n_E}{n_I} \right) \left(\frac{T_E}{T_I} \right)^{1/2} \left(\frac{m_I}{m_E} \right)^{1/2} \approx 25 \quad (12)$$

For the 25 events studied, the ratio J_{EO}/J_{IO} is actually 24 ± 7 . As the current ratio enters as a logarithm, Eq. (11) becomes:

$$|qV_o| \approx T_E \ln(2.5) \approx T_E . \quad (13)$$

In Figure 2, the electron temperature (assumed to be Maxwellian) is plotted versus the observed potential. An expression linear in the ambient temperature was fit to the data by the least squares method (the two marked points were not included as the plasma is believed to have changed between the measurement of

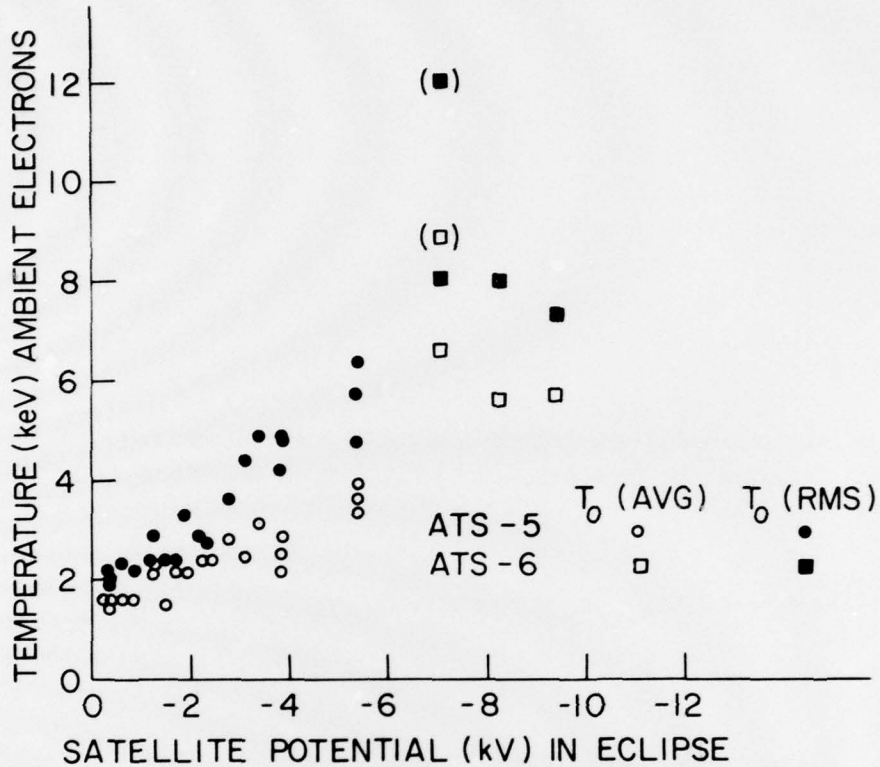


Figure 2. The Observed Temperature of the Ambient Electrons vs the Satellite Potential in Eclipse. T_o (AVG) is given by 2/3's of the ratio of the energy density to the number density. T_o (RMS) is given by 1/2 of the ratio of the energy flux to the number flux. The difference between these two temperatures is a measure of the adequacy of a Maxwellian approximation

T_E and the potential). Depending on which definition of the temperature is used the fits and correlation coefficients are:

$$V_o^* = 1391 - 1.63 T_E(\text{AVG}) \quad (r = 0.86) \quad (14)$$

$$V_o^* = 1828 - 1.29 T_E(\text{RMS}) \quad (r = 0.92)$$

These relationships not only demonstrate the validity of Eq. (13), but imply the existence of a threshold electron temperature above which the satellite potential is linear. Such behavior, though not explicit in our simple theory, is due to the fact that at an intermediate energy (usually a few hundred eV), the secondary yield is

greater than 1 (Rubin et al⁷). The electron temperature must be several times greater than this threshold energy before significant charge buildup occurs.

4. POTENTIAL DURING ECLIPSE PASSAGE

As a spacecraft enters and exits the earth's penumbra, it sees a varying illumination generating a varying photoelectron current as the sun's disc is obscured by the limb of the earth. The percentage of solar illumination as a function of X_m seen by a satellite at geosynchronous orbit is plotted in Figure 3 (the attenuation function is based on the work of Garrett⁹ and, as the details are not of concern to this generalized treatment, the reader is referred to that paper). Dividing Eq. (7) by Eq. (8):

$$\frac{V(X_m)}{V_o} = \frac{\ln[(y/x)(J_{IO}/J_{EO})(1 + |qV|/T_I) + 1/x(J_{PO}/J_{EO}) f(X_m)]}{\ln[(y/x)(J_{IO}/J_{EO})(1 + |qV_o|/T_I)]} \quad (15)$$

Estimating as before and, as $|qV| \lesssim |qV_o|$:

$$\frac{V(X_m)}{V_o} \approx -\ln[.4 + 2.5 (J_{PO}/J_{EO}) f(X_m)] \quad (16)$$

The ratio J_{PO}/J_{EO} is not known accurately as it is a function of the material and structure of the spacecraft. From Whipple,² Grard et al,⁸ DeForest,¹ and Garrett,⁹ a reasonable range of values is:

$$1.6 \lesssim J_{PO}/J_{EO} \lesssim 16 \quad (17)$$

7. Rubin, A. G., Rothwell, P. L., and Yates, G. K. (1978) Reduction of spacecraft charging using highly emissive surface materials, Proc. 1978 Symposium on the Effect of the Ionosphere on Space and Terrestrial Systems, Naval Research Lab., Washington D. C.
8. Grard, R. J. L., Knott, K., and Pedersen, A. (1973) The influence of photo-electron and secondary electron emission on electric field measurements in the magnetosphere and solar wind, Photon and Particle Interactions with Surfaces in Space, R. J. C. Grard (Ed.), D. Reidel Publishing Co., Dordrecht, Holland, pp. 163-189.
9. Garrett, H. B. (1978) Effects of a Time-Varying Photoelectron Flux on Space-craft Potential, AFGL-TR-78-0119.

In Figure 3, Eq. (16) is plotted for $f(X_m)$ given by Garrett⁹ and for $J_{PO}/J_{EO} = 1.6$ and 16. Also shown are data from ATS-5 and ATS-6 for the 25 eclipse passages. The observations are subject to a large (~ 25 km) error in X_m , as the orbits of ATS-5 and ATS-6 were not updated sufficiently often to allow a more accurate position determination (Garrett⁹). Even so, the predicted variation in parameters brackets the actual observations.

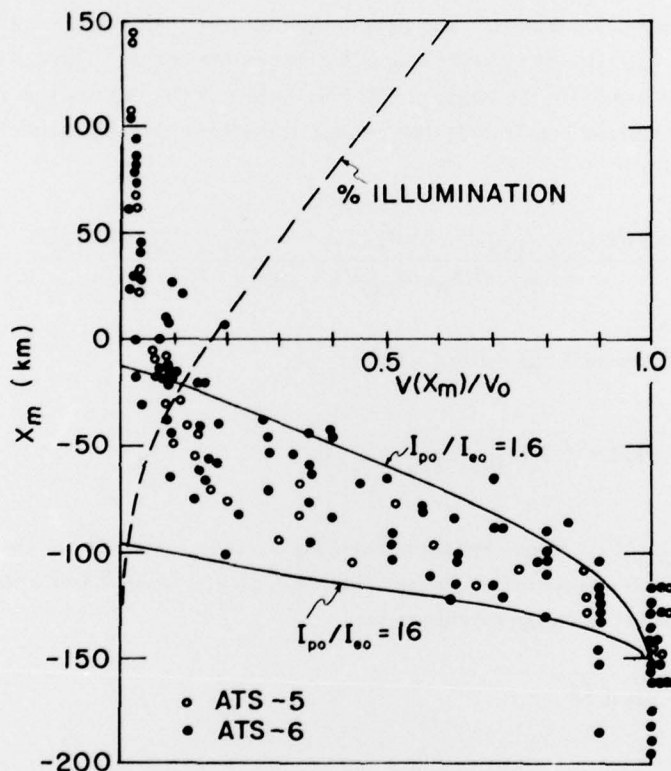


Figure 3. The Ratio of the Varying Potential to the Maximum Potential When the Spacecraft Were in Eclipse. Also shown are the percent illumination (same scale as $V(X_m)/V_0$) and the predicted curves for I_{po}/I_{eo} values of 1.6 and 16

5. DISCUSSION

In the previous sections, we have presented equations (Eq. (13) and (16)) that approximate ATS-5 and ATS-6 observations of the varying potential that exists between the spacecraft and the ambient plasma. We believe that this is primarily the result of the rough constancy of the ratio J_{IO}/J_{EO} and the fact that variations in this ratio enter as a logarithm. Further, it is tacitly assumed that T_I and T_E , the Maxwellian temperatures, have meaning. Although these assumptions are not valid at all times at geosynchronous orbit (particularly at quiet times when non-Maxwellian ring currents are observed), they are adequate following plasma injections when a satellite is near midnight. As this is a prerequisite for charging to occur during eclipse passage, Eqs. (13) and (16) are valid.

Equations (13) and (16) are of use in many space physics problems. As an example, given T_E , the potential in eclipse can be estimated by Eq. (13). Equivalently we have plotted the frequency of occurrence of potentials in eclipse for ATS-5 and ATS-6 for 4 years. With Figure 4 and Eq. (16), the occurrence frequency of various potential levels as the spacecraft entered into eclipse can be estimated for the same 4 year period (Rubin and Garrett¹⁰). As ATS-5 is a spinning cylindrical shape (1.3 m in diameter by 2 m in length) and ATS-6 is a large (10 m) spin-stabilized dish antenna, the equations are also applicable to a variety of problems and simple space structures. For instance, by equating the photoelectron current to an electron beam, Eq. (13) and (16) can be used to simulate the effects of a varying electron beam.

Although the scaling to large space structures may not be completely valid, the results of Eq. (13) and (16) may be used in principle to estimate the potential that would exist between the ends of a large space structure. This can be most readily visualized by assuming the structure to be approximated by two spheres separated by a distance equal to that of the structure, and connected by a long cable having the electrical loading characteristics of the structure. For infinite resistance, Eqs. (13) and (16) can be used to estimate the potential on each sphere as it passes into eclipse. Assuming the distance between the two spheres to be equal to their difference in X_m , the potential difference between the two ends can be estimated as they pass into eclipse. Depending on the exact nature and size of the structure, this simple analogy would predict potentials as high as -20,000 V, a clear hazard to the spacecraft.

10. Rubin, A. G., and Garrett, H. B. (1978) A Statistical Study of Eclipse Potentials for ATS-5 and ATS-6, to appear as AFGL In-House Report.

In conclusion, elementary probe theory suggests basic relations between the electron temperature (assumed Maxwellian) and the spacecraft potential relative to the ambient plasma when the spacecraft is in the earth's shadow. Relations describing the potential variations as the spacecraft passes into eclipse are derived. Observations from ATS-5 and ATS-6 support these derivations and indicate that the reason for agreement, is because the ratio of the ambient ion to electron current is roughly constant for injection events and enters as a logarithm. Provided that the results are of general applicability, they can be used to estimate the potentials on large space structures and the effects of electron beams.

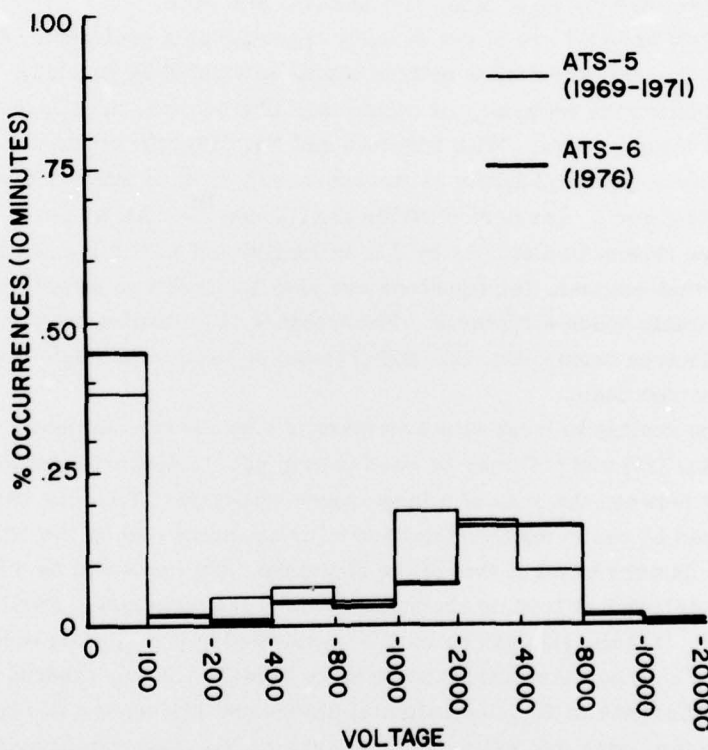


Figure 4. The Occurrence Frequency of Eclipse Potentials for ATS-5 and ATS-6. 10 minute averages were employed

References

1. DeForest, S. E. (1972) Spacecraft charging at synchronous orbit, J. Geophys. Res. 77:651-659.
2. Whipple, E. C. (1965) The Equilibrium Electric Potential of a Body in the Upper Atmosphere, NASA X-615-65-296.
3. Chen, F. F. (1965) Electric Probes, Plasma Diagnostic Techniques, R. H. Huddlestone and S. L. Leonard (Ed.), Academic Press, Inc., New York, pp. 113-200.
4. DeForest, S. E., and McIlwain, C. E. (1971) Plasma clouds in the magnetosphere, J. Geophys. Res. 76:3587-3611.
5. Mauk, B. H., and McIlwain, C. E. (1975) ATS-6 UCSD auroral particles experiment, IEEE Trans. Aerospace and Electronic Systems, AES-11(No. 6): 1125-1130.
6. Garrett, H. B. (1978) Spacecraft Potential Calculations - A Model, AFGL-TR-78-0116.
7. Rubin, A. G., Rothwell, P. L., and Yates, G. K. (1978) Reduction of spacecraft charging using highly emissive surface materials, Proc. 1978 Symposium on the Effect of the Ionosphere on Space and Terrestrial Systems, Naval Research Lab., Washington D.C.
8. Grard, R. J. L., Knott, K., and Pedersen, A. (1973) The influence of photo-electron and secondary electron emission on electric field measurements in the magnetosphere and solar wind, Photon and Particle Interactions with Surfaces in Space, R. J. C. Grard (Ed.), D. Reidel Publishing Co., Dordrecht, Holland, pp. 163-189.
9. Garrett, H. B. (1978) Effects of a Time-Varying Photoelectron Flux on Space-craft Potential, AFGL-TR-78-0119.
10. Rubin, A. G., and Garrett, H. B. (1978) A Statistical Study of Eclipse Potentials for ATS-5 and ATS-6, to appear as AFGL In-House Report.